agriculture

MDPI

Article

The Effects of Biochar Application Duration on N_2O Emissions and the Species and Functions of Nitrifying and Denitrifying Microorganisms in Paddy Soils

Zhongcheng Zhang [1,†], Xue Lan [1,†], Kai Zhang [1], Jinrui Zhao [1], Yanghui Sui [2], Xinyue Bing [1], Zhongcheng Sun [1], Jialing Wang [1], Wenzhong Zhang [1] and Jiping Gao [1,*]

[1] Rice Research Institute, National and Local Joint Engineering Laboratory of Japonica Rice Breeding and Cultivation Technology in North China, Shenyang Agricultural University, Shenyang 110866, China
[2] Corn Research Institute, Liaoning Academy of Agricultural Sciences, Shenyang 110161, China; suiyanghui@126.com
* Correspondence: jipinggao@syau.edu.cn
† These authors contributed equally to this work.

Abstract

Further understanding is needed regarding how biochar, over the long term, influences N_2O release and the associated communities of nitrifiers and denitrifiers in paddy soils. This field study examined the responses of these microbial communities to biochar applied for different durations (2016 or 2023) and at different doses (15 or 45 t·ha^{-1}), alongside a control (CK) without biochar addition. Relative to the control (CK), all biochar amendments led to a comprehensive enhancement of soil physicochemical properties. However, their impacts on N_2O fluxes diverged: cumulative emissions rose by 18.44% under the high-rate (45 t·ha^{-1}), first-year application (NB45) in 2023, but were suppressed across all other biochar treatments. Microbial community composition diverged markedly between treatment chambers, with the abundances of *Nitrospira* and Chloroflexota showing distinct patterns. In 2016, the two bacterial species exhibited significantly high abundance proportions, with maximum shares of 23.55% (2016, 45 t·ha^{-1}) and 12.16% (2016, 45 t·ha^{-1}), the most abundant in nitrification and denitrification, respectively, which influenced the certainty of changes in the microbial community structure. Biochar enhances nitrogen metabolism in nitrifying microorganisms but inhibits denitrification processes, with the biochar applied in 2023 having a remarkable effect. Overall, biochar application effectively enhances soil physicochemical properties, mitigates N_2O emissions over the long term, and modulates the community structure and functional traits of nitrifying and denitrifying microorganisms. These combined effects contribute to promoting environmental security for sustainable development within agricultural production systems while reducing the carbon footprint.

Keywords: rice paddy; duration of biochar application; N_2O emissions; nitrifying microorganisms; denitrifying microorganisms

Check for updates

Academic Editor: Dominika Lewicka-Szczebak

Received: 31 December 2025
Revised: 5 February 2026
Accepted: 9 February 2026
Published: 13 February 2026

Copyright: © 2026 by the authors. Licensee MDPI, Basel, Switzerland. This article is an open access article distributed under the terms and conditions of the Creative Commons Attribution (CC BY) license.

1. Introduction

Global climate change is intensifying, presenting ever more significant challenges. As one of the core factors in climate change, greenhouse gas (GHG) emission reduction has become a key factor in coping with global warming [1,2]. The year 2024 saw global atmospheric concentrations of 423 ppm for CO_2 (carbon dioxide), 1932 ppb for CH_4 (methane),

and 338 ppb for N_2O (nitrous oxide) [3,4]. Notably, although the concentration of N_2O is relatively low, in terms of the greenhouse effect, its global warming potential (GWP) is as high as 298 times that of an equivalent amount of CO_2, and it depletes the ozone layer [5,6]. Globally, nearly 84% of N_2O emissions originate from agricultural production. Rice cultivation significantly contributes to agricultural N_2O emissions, with N_2O emissions from nitrification and denitrification in rice paddies accounting for approximately 11% of the total global agricultural emissions [7–9]. Therefore, methods to reduce N_2O emissions from rice planting have become an increasingly important focus area of research.

The emission of N_2O from soil is mainly due to microbe-mediated nitrification and denitrification [10]. Nitrification is performed by *Nitrosomonas* and *Nitrobacter* via an oxidation pathway [11]. Under aerobic conditions, ammonia-oxidizing archaea (AOA) and ammonia-oxidizing bacteria (AOB) gradually convert NH_4^+ to NO_3^- through the ammonia oxidation pathway. Under anoxic conditions, soil AOB can reduce NO_2^- to N_2O through both nitrification and denitrification pathways [12,13]. In long-term flooded paddy soils, N_2O is primarily produced through denitrification, which contributes approximately 70% of the N_2O emissions from paddy fields [14,15]. Denitrification sequentially reduces nitrate (NO_3^-) to nitrite (NO_2^-), nitric oxide (NO), and N_2O, ultimately producing nitrogen gas (N_2). This process is catalyzed by napA/narG (nitrate reductase), nirK/nirS (nitrite reductase), norB (nitric oxide reductase), and nosZ (nitrous oxide reductase) [16]. The abundance of these genes and the structure of microbial communities can serve as potential indicators for predicting N_2O emissions [17]. Thus, investigating changes in key gene abundance and microbial community structure provides critical guidance for developing strategies to mitigate N_2O emissions.

Produced through the pyrolysis of organic feedstocks under oxygen-limited conditions, biochar is a carbonaceous material characterized by its high stability and porosity. Its distinct porous architecture and physicochemical attributes confer multiple benefits for soil amelioration and hold potential for reducing the release of greenhouse gases (GHGs) [18,19]. This material optimizes aeration conditions by increasing soil porosity and improving soil aggregation. Owing to its physical adsorption properties and high carbon-to-nitrogen ratio, it can adsorb NH_4^+ and fix NO_3^-, thereby inhibiting N_2O emissions [18,20]. Applying biochar to rice paddy soils can increase pH, water retention, and overall nutrient content, thereby improving the soil environment and promoting the N cycle. It can also reduce the adsorption of ammonium nitrogen by the soil, further reducing the ammonium nitrogen content and promoting the conversion of nitrate-nitrogen [21,22]. Biochar can increase enzyme activity in the soil and optimize microbial activity and diversity [22,23]. Biochar promotes the expression of the nosZ gene by raising soil pH, increasing nitrous oxide reductase concentration, accelerating the conversion of N_2O to N_2, and reducing N_2O emissions [24]. A previous study demonstrated that adding biochar to soil significantly affects the abundance of nirS and nirK-type denitrifying bacteria and that the activities of these denitrifying bacteria can also influence N_2O emissions [25]. Moreover, biochar is known to reduce N_2O formation by decreasing the abundance of fungal nirK, AOB, and amoA genes and increasing the abundance of nosZI and nosZII genes [26]. Biochar also inhibits fungal denitrification by increasing soil pH and altering fungal community composition [27]. Changes in pH are also related to the abundance and community changes in AOB. A synthesis of existing studies indicates that biochar influences N_2O emissions in the soil denitrification pathway by regulating the bacterial and fungal community structures. However, there is a lack of research on how the long-term effects (over multiple years) on soil affect the structure of the microbial community after biochar application.

We hypothesized that biochar applied at different durations and rates could continuously regulate the physical and chemical properties of the soil to varying degrees. Additionally, by regulating the microbial species and functions related to nitrification and denitrification in paddy fields, this study aimed to explore their effects on N_2O emissions. From a soil microecosystem perspective, we explored the significance of biochar applied in different years in reducing N_2O emissions in paddy fields, the enhancement effects of biochar on paddy soil fertility, and its potential for GHG reduction. We aimed to provide theoretical support for its scientific application in agriculture.

2. Materials and Methods

2.1. Field Site Characteristics and Materials

The field experiment was located at the experimental station of the Rice Research Institute (RRI, Shenyang Agricultural University, SYAU), located at 123°34′38.82″ E, 41°49′34.15″ N. This study utilizes a field-based biochar experiment initiated in 2016, which has been maintained as a long-term trial. All sample collection activities were concentrated in 2023. The experimental site experiences a temperate continental monsoon climate, characterized by moderately fertile brown soils and flat terrain. Key baseline soil properties (2016) included: pH, 6.3; bulk density, 1.32 $g \cdot cm^{-3}$; soil organic matter (SOM), 15.35 $g \cdot kg^{-1}$; and total nitrogen (TN), 0.96 $g \cdot kg^{-1}$. Additionally, available concentrations of N, P, and K measured 63.70, 17.90, and 70.30 $mg \cdot kg^{-1}$. The biochar used, derived from corn stover through pyrolysis at 400 °C, was supplied by the Liaoning Provincial Biochar Engineering Technology Research Center. The biochar properties were: pH, 9.90; electrical conductivity (EC), 17.9 $m \cdot S \cdot cm^{-1}$; total carbon (TC), 274.4 $g \cdot kg^{-1}$; total nitrogen (TN), 6.40 $g \cdot kg^{-1}$. It also provided 110 $mg \cdot kg^{-1}$ of alkali-hydrolysable N, along with available P and K at 780 $mg \cdot kg^{-1}$ and 20.9 $g \cdot kg^{-1}$. The fertilizers applied were urea at 46% N, superphosphate at 12% P_2O_5, and potassium chloride at 60% K_2O.

The rice cultivar employed was 'Beijing 1501'. This variety was developed at the RRI of SYAU. It is characterized by robust stems, well-developed root systems, compact plant structure, and upright panicles. These morphological features facilitate the collection and observation of GHGs.

2.2. Experimental Design and Treatments

A completely randomized block design was employed for this study. Biochar amendments were applied to the rice fields in two distinct phases: initially in April 2016 (termed FB) and again in April 2023 (termed NB). The biochar application rates were set at 0, 15, and 45 $t \cdot ha^{-1}$. The experiment included five treatments: (i) FB15 and (ii) FB45, receiving 15 and 45 $t \cdot ha^{-1}$ of biochar in April 2016, respectively; (iii) NB15 and (iv) NB45, receiving 15 and 45 $t \cdot ha^{-1}$ in April 2023, respectively; and (v) CK, which served as the control without biochar application. There are a total of five treatments, each with three replicates. A total of 15 plots were laid out. The individual plot size was 3.0 m in width and 3.3 m in length. Additionally, black rigid plastic barriers buried 25 cm deep were installed around each plot to effectively prevent the lateral movement of water and fertilizer. Chemical fertilizers were applied following a standardized protocol. Nitrogen fertilizer (total amount: 210 $kg \cdot ha^{-1}$) was allocated in a ratio of 3.6:2.4:4 applied as a base fertilizer, tillering fertilizer, and heading fertilizer during the three critical growth stages. Potassium fertilizer was applied at 180 $kg \cdot ha^{-1}$ in total. This amount was divided equally, with half applied as a basal dose and the remainder top-dressed at the tillering stage. Phosphorus fertilizer (180 $kg \cdot ha^{-1}$) was placed entirely as a basal dose. All remaining field management practices were consistent with standard high-yield cultivation practices. The entire experimental

cycle from sowing to harvest lasted approximately five and a half months, specifically: sowing on 23 April, transplanting on 27 May, and harvesting on 7 October.

Biochar application rates were set at 15 and 45 t·ha^{-1}. The 15 t·ha^{-1} rate referenced optimal application recommendations for crop residue biochar in Northeast China. Since uncertainty significantly increases at application rates exceeding 40 t·ha^{-1}, the high rate of 45 t·ha^{-1} aimed to explore the potential upper limit of biochar effects and establish a clear dose–response relationship [28]. All biochar was applied in a single application during the April rice field tillage, ensuring agronomic feasibility and providing a buffer period for the stabilization of biochar in the soil.

2.3. Collecting and Analyzing Samples

Continuous measurements of GHG emissions were obtained using a static acrylic chamber fitted with heat-insulating aluminum foil. The dimensions of the lightbox were 0.5 m × 0.3 m × 0.7 m. When rice plants grew taller than the container, an extension box of identical dimensions but 0.3 m in height, with openings on both sides at the base, was used. Each enclosure featured a battery-powered 12 V fan mounted on the inner top surface to mix the gases. The pre-installed recessed bases (flush with the floor) in each compartment ensured a sealed fit when the enclosures were placed. GHGs were placed five days after rice transplantation. Sampling GHG was conducted throughout the rice growing season, within the morning window of 08:00–11:00, and only on rain-free days. Sampling was performed every seven days, and an additional collection was performed three days post-fertilization. Gas sampling was performed at intervals of 0, 10, 20, and 30 min by withdrawing air from the chamber headspace with a 50 mL syringe. These samples were then directly transferred to 100 mL aluminum foil vacuum bags and sealed for preservation. Following collection, all vacuum bag samples underwent quantitative analysis of N_2O concentrations in the laboratory. This analysis was performed using a greenhouse gas analyzer equipped with a hydrogen ionization detector (Agilent 7890 B, serial number 18001268S, Agilent Technologies Inc., Santa Clara, CA, USA).

N_2O emission fluxes were derived from static chamber observation data using the following formula [29]:

$$F = \rho \times \frac{V}{A} \times \frac{dc}{dt} \times \frac{273}{273 + T} \quad (1)$$

where ρ is the standard N_2O density (1.25 g·L^{-1}); V and A correspond to the effective chamber volume (m^3) and base area (m^2), respectively; dc/dt indicates the linear rate of concentration increase for N_2O in the headspace (μL·L^{-1}·h^{-1}); and T is the mean sampling temperature (°C) inside the chamber.

To estimate total seasonal N_2O emissions, the following equation was employed [30]:

$$T = \sum \frac{F_{i+1} + F_i}{2} \times D_{i+1} - D_i \times 24 \quad (2)$$

where T signifies cumulative seasonal N_2O emissions, expressed in kg·ha^{-1}. F_i and F_{i+1} refer to the mean N_2O flux (mg·m^{-2}·h^{-1}) corresponding to the *i*-th and the (*i* + 1)-th sampling intervals, respectively. D_i and D_{i+1} stand for the dates (in days) of these two consecutive sampling events. The total N_2O emissions were determined by averaging the results from four replicate observations and weighting them according to the time intervals between observations.

Soil sampling was conducted at rice heading by collecting composites from five points within the 0–20 cm layer of each plot. Sampling was performed with an auger under flooded conditions. Homogenized samples were bagged in sterile plastic, flash-frozen on dry ice, and expedited to the laboratory for cryopreservation at −80 °C prior to DNA extraction.

2.4. Sequencing and Analysis of Metagenomic DNA

2.4.1. Genomic DNA Extraction

Shanghai Meiji Biotechnology Co., Ltd. (Shanghai, China) was commissioned to perform the subsequent processing, encompassing DNA isolation and Illumina-based sequencing. The detailed protocol is described below. First, the MJ-faeces soil DNA extraction kit (Shanghai MajorbioYuhua Bio-pharm Technology Co., Ltd., Shanghai, China) was used to extract the sample DNA. DNA quality was assessed by measuring concentration and purity (NanoDrop2000, Thermo Fisher Scientific, Waltham, MA, USA, and TBS-380, Turner Biosystems Inc., Sunnyvale, CA, USA) and confirming integrity via 1% agarose gel electrophoresis. Subsequently, an aliquot was sheared to approximately 350 bp fragments using a Covaris M220 (Covaris Inc., Woburn, MA, USA) ultrasonic homogenizer in preparation for paired-end (PE) library construction.

2.4.2. Construction of Libraries for Illumina Sequencing

Library preparation was conducted with the NEXTFLEX® Rapid DNA-Seq Kit (Bioo Scientific, Austin, TX, USA). First, magnetic bead screening was performed to eliminate self-connecting segments at the joints. Subsequently, PCR was carried out to amplify the library templates. Magnetic beads were used to purify the PCR products, and the resulting material constituted the final library for sequencing. Following library preparation, Shanghai Meiji Biotechnology Co., Ltd. was commissioned to carry out the metagenomic sequencing on an Illumina NovaSeq system. The sequencing principle is as follows: first, library molecules bind to complementary bases on one end of a fixed primer, are amplified, and are attached to the chip. Subsequently, the other end binds to a nearby primer to form a 'bridge'. This bridge is then amplified by PCR, yielding the DNA clusters. Following linearization to generate single-stranded amplicons, the reaction mixture was supplemented with modified DNA polymerase and four-color fluorescent dNTPs. Every synthesis cycle was limited to the incorporation of a single nucleotide. The identity of nucleotides incorporated in the initial cycle was read out by scanning the plate surface with a laser. Subsequently, chemical cleavage removed the 'fluorescent group' and 'terminator group', restoring extension activity at the 3′-end to enable the next round of nucleotide polymerization. Continuous recording of fluorescence emission from each sequencing cycle enabled the assembly of complete template DNA sequences.

2.4.3. Analytical Methods

To obtain high-quality sequences, raw reads were subjected to preprocessing with Fastp (version 0.23.0) [31]. Reads below the thresholds (length < 50 bp, average quality < 20, or containing N bases) were eliminated, retaining qualified paired-end and single-end reads. MEGAHIT (version 1.1.2) software [32] was employed for sequence assembly based on the compact De Bruijn graph algorithm. The optimized sequences were assembled using the MEGAHIT software based on the principle of compact De Bruijn graphs. The final assembly was constructed using contigs with a minimum length of 300 bp. Subsequently, ORF prediction was performed on the resulting contigs using Prodigal [33]/MetaGene [34] (version 2.6.3). Genes meeting the length threshold (≥100 bp) were selected and subsequently subjected to translation to derive the amino acid sequences.

For gene sequence clustering across all samples, the CD-HIT (version 4.6.1) program [35] was utilized. Clustering was based on a 90% identity and 90% coverage standard, resulting in a non-redundant gene catalog. This study then employed SOAPaligner (version 2.21) [36] for the subsequent step. Using this software to quantify gene abundance, reads from every sample were mapped to the non-redundant set using a 95% identity cutoff. Based on this alignment, the gene abundance corresponding to each sample was statistically determined. A homology search was carried out with DIAMOND (version 0.8.35) [37], aiming to achieve species classification and functional predictions. The search compared the gene-derived amino acid sequences to the NR, KEGG, and COG databases under BLASTP settings (e-value: 1×10^{-5}). Based on the abundance of the gene sets, the relative abundances of both functions and species were then determined.

2.5. Data Processing

IBM SPSS Statistics software package (version 27.0.1) was used to perform one-way analysis of variance (ANOVO). Multiple comparisons of means were conducted at the $p < 0.05$ level using the Least Significant Difference (LSD) method. Graphical representation of GHGs flux dynamics was generated with Origin 2022. Metagenomic data were visualized using the Meiji Cloud platform, which included principal coordinate analysis (PCoA) based on Bray–Curtis distance. ANOSIM was performed to assess intergroup differences. All graphical elements were integrated with Adobe Photoshop 2023.

3. Results

3.1. Soil Physicochemical Parameters

Analysis of key soil properties was conducted on samples collected at the full heading stage across all treatments (Figure 1a,e). Relative to CK, elevated SOM levels were observed in plots that received biochar, whether applied in the first or the eighth year. Specifically, the treatments with NB15 and NB45 significantly increased the SOM content by 34.75% and 55.26%, respectively. Under the same biochar application duration, the SOM content under the high biochar application rate was higher than that under the low biochar application rate; however, no significant difference was observed. As shown in Figure 1b,f, the soil pH changed significantly. Except for the FB15 (6.83 ± 0.02) treatment, the NB45 (7.55 ± 0.05), NB15 (7.07 ± 0.02), and FB45 (7.04 ± 0.03) treatments significantly increased soil pH by 11.52%, 4.43%, and 3.99%, respectively, compared with CK (6.77 ± 0.02). For the same duration of biochar application, the pH under the high biochar application rate was higher than that under the low biochar application rate. Significant changes were observed in the soil content of nitrate nitrogen (NO_3^-–N), as presented in Figure 1c. A peak value of 13.85 ± 0.30 mg·kg^{-1} was recorded in the CK treatment, which was the highest among all treatments. Under NB, higher biochar rates led to increased NO_3^-–N content. In contrast, FB conditions resulted in lower NO_3^-–N content with increased biochar application. However, all were reduced by more than 50% compared to CK. As shown in Figure 1d, there were evident differences in the content of ammonium nitrogen (NH_4^+–N) in the soil. The content under the CK treatment was the highest, reaching 9.22 ± 0.83 mg·kg^{-1}. Compared with the CK treatment, all other treatments showed significant differences, with reductions exceeding 30%. Under the FB conditions, the NH_4^+–N content was significantly higher in the low biochar application treatment than in the high biochar application treatment. The same trend was observed under NB conditions; however, the difference was not significant.

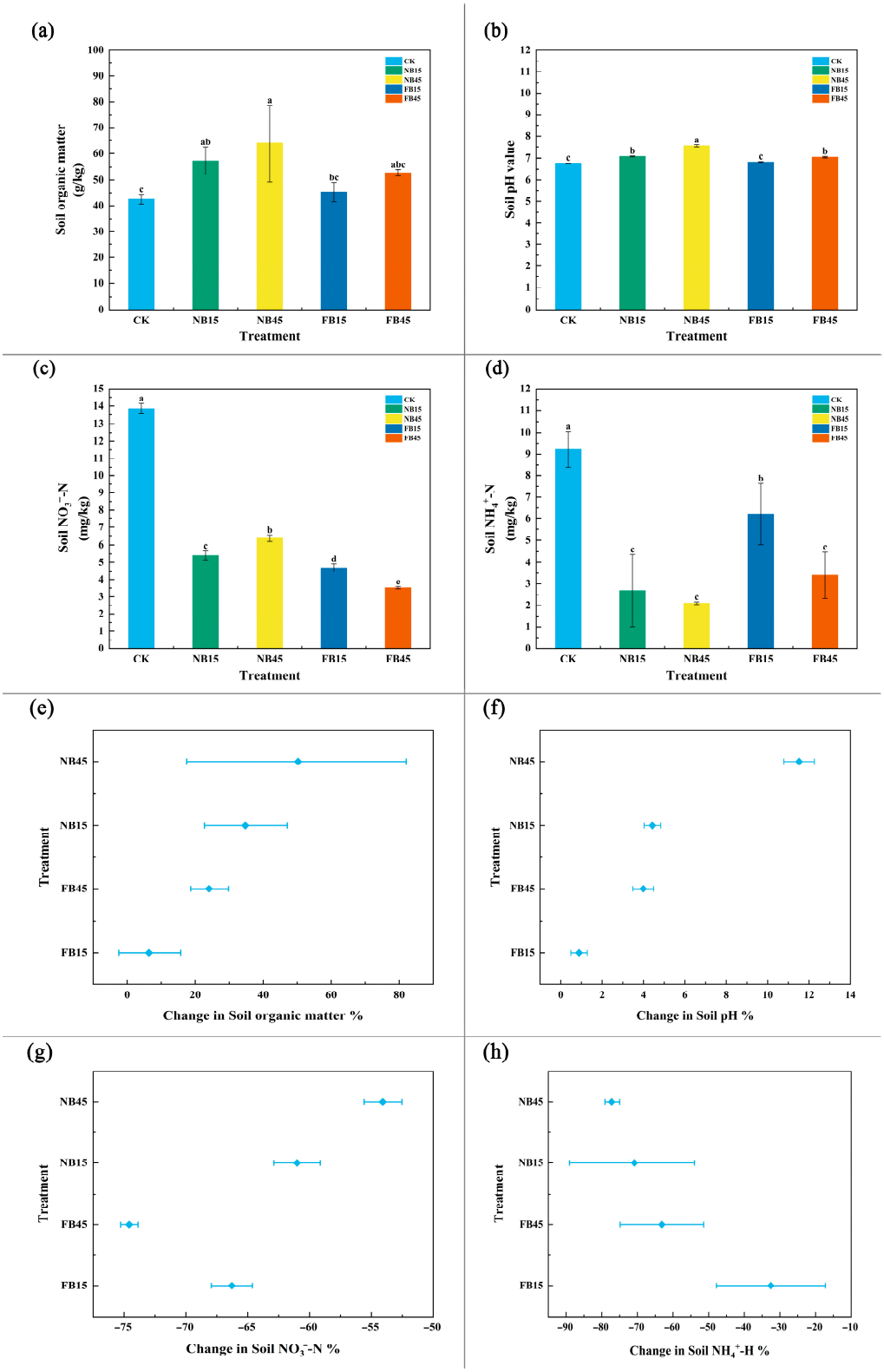


Figure 1. Duration-dependent alterations in paddy soil attributes following biochar addition (**a**): Soil Organic Matter (SOM), (**b**): pH, (**c**): Nitrate Nitrogen (NO_3^-–N), (**d**): Ammonium Nitrogen (NH_4^+–N). Relative change rates (%) in physicochemical properties of paddy soil after biochar application compared to the control group: (**e**): SOM, (**f**): pH, (**g**): NO_3^-–N, (**h**): NH_4^+–N. Data points (diamonds) represent the mean, while error bars denote the 95% confidence interval. CK: unamended control; FB15 & FB45: received 15 or 45 t·ha^{-1} biochar in the 8th year (FB); NB15 & NB45: received 15 or 45 t·ha^{-1} biochar in the 1st year (NB). Different lowercase letters above the bar charts indicate significant differences at the $p < 0.05$ level ($n = 3$).

3.2. N_2O Emissions from Paddy Fields

This study monitored and recorded the N_2O emission flux dynamics of all treatments throughout the rice growth period (Figure 2a). The overall emission trends were similar, showing two regular increases followed by decreases and two emission peaks during the monitoring period. After the second fertilization, the first emission peak occurred on the 33rd day after transplantation. For all the treatments, the magnitude relationship was NB45 (0.9439 ± 0.06) > CK (0.5092 ± 0.05) > FB45 (0.5006 ± 0.05) > FB15 (0.4595 ± 0.01) > NB15 (0.2864 ± 0.02). The unit of measurement was ($mg \cdot m^{-2} \cdot h^{-1}$). On the 61st day after transplantation, corresponding to the period after the third fertilization, a second peak in N_2O flux occurred. The emission flux under the CK treatment peaked at 0.9339 ± 0.07 $mg \cdot m^{-2} \cdot h^{-1}$, representing the highest value among all treatments. The N_2O emission flux from the NB45 treatment ranked second among all treatments, surpassed only by the CK treatment. The emission flux under the FB45 treatment fluctuated slightly, being 0.2675 ± 0.01 $mg \cdot m^{-2} \cdot h^{-1}$.

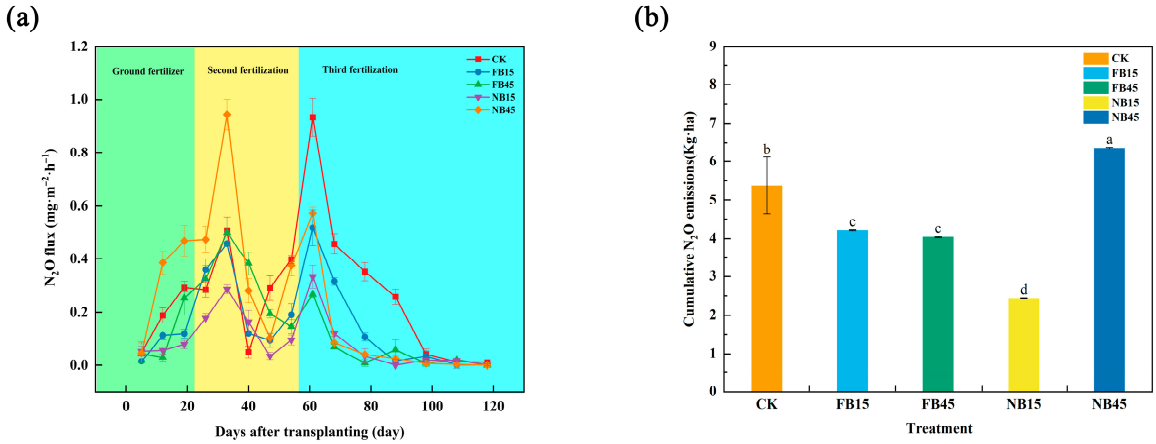


Figure 2. Effects of the application duration of biochar on the N_2O emission flux (**a**) and the cumulative N_2O emissions (**b**) in paddy fields. CK: unamended control; FB15 & FB45: received 15 or 45 $t \cdot ha^{-1}$ biochar in the 8th year (FB); NB15 & NB45: received 15 or 45 $t \cdot ha^{-1}$ biochar in the 1st year (NB). Different lowercase letters above the bar charts indicate significant differences at the $p < 0.05$ level ($n = 3$).

Figure 2b presents the cumulative N_2O emissions over the entire rice growing season. The NB45 treatment had the highest cumulative emissions, reaching 6.36 ± 0.16 $kg \cdot ha^{-1}$. Compared with the CK (5.37 ± 0.15 $kg \cdot ha^{-1}$) treatment, the cumulative emissions increased by 18.44%. Compared with the CK treatment, the FB15 (4.22 ± 0.12 $kg \cdot ha^{-1}$) and FB45 (4.04 ± 0.16 $kg \cdot ha^{-1}$) treatments reduced cumulative N_2O emissions by 21.42% and 24.77%, respectively. Relative to the CK treatment, the NB15 treatment exhibited the lowest cumulative emissions (2.44 ± 0.09 $kg \cdot ha^{-1}$), a decrease of 54.56%.

3.3. Analysis of Microbial Species Involved in Nitrification and Denitrification in Paddy Field Soil

As shown in Figure 3a, the species analysis of microorganisms related to nitrification was conducted at the genus level. The microorganisms involved in nitrification were bacteria (5.30%), archaea (94.53%), and unclassified microorganisms (0.17%). The four most abundant bacterial groups were *Nitrospira*, Chloroflexota, *Anaeromyxobacter*, and Deltaproteobacteria. The abundance of the dominant bacterial groups varied among the treatments. *Nitrospira* accounted for 17.44%, 11.66%, 6.46%, 20.42%, and 23.55% of the CK, NB15, NB45, FB15, and FB45 treatments, respectively. After conducting a multiple-group comparative analysis of *Nitrospira* (Figure 3b), its relative abundance in the NB45 treatment was significantly lower than that in the CK treatment ($p < 0.01$). At the same biochar application rate, a significant downward trend in *Nitrospira* abundance was observed in

the NB15 treatment relative to the FB15 treatment ($p < 0.05$). This trend was more pronounced at the 45 t·ha^{-1} biochar application rate, where the NB45 treatment exhibited a highly significant decrease compared with that of the FB45 treatment ($p < 0.001$). The proportions of Chloroflexota in the CK, NB15, NB45, FB15, and FB45 treatments were 9.54%, 13.57%, 13.79%, 11.97%, and 9.26%, respectively. In the multiple-group comparison (Figure 3c), the NB45 and FB45 treatments differed significantly in the relative abundance of Chloroflexota, with NB45 showing a greater abundance ($p < 0.05$). *Anaeromyxobacter* accounted for 6.17%, 8.70%, 10.14%, 6.06%, and 5.68% of the CK, NB15, NB45, FB15, and FB45 treatments, respectively. No significant difference was observed between the treatments (Figure 3d). When comparing the abundance of Deltaproteobacteria among all treatments, the FB45 treatment had the highest proportion, reaching 7.89%, whereas the NB45 treatment had the lowest proportion (3.72%). At the 45 t·ha^{-1} biochar rate, NB conditions resulted in a significantly lower ($p < 0.01$) proportion of Deltaproteobacteria compared to FB conditions (Figure 3e).

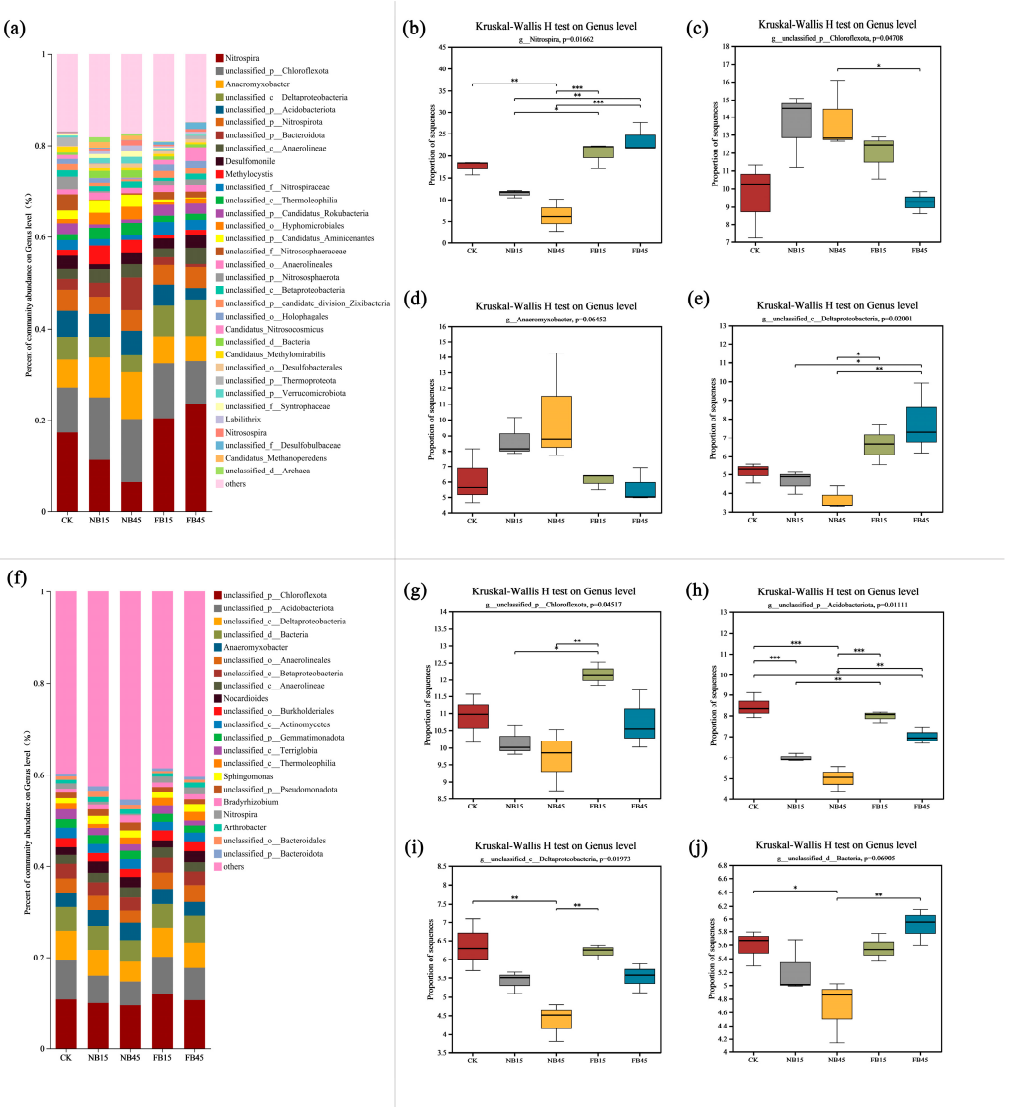


Figure 3. Community composition of nitrifying (**a**) and denitrifying (**f**) microorganisms at the genus level and comparison of differences among groups of the top four dominant species of nitrifying (**b**–**e**) and denitrifying (**g**–**j**) microorganisms. CK: unamended control; FB15 & FB45: received 15 or 45 t·ha^{-1} biochar in the 8th year (FB); NB15 & NB45: received 15 or 45 t·ha^{-1} biochar in the 1st year (NB). *: significant at $p < 0.05$; **: significant at $p < 0.01$; ***: significant at $p < 0.001$.

As shown in Figure 3f, species analysis of denitrification-related microorganisms was conducted at the genus level. The microorganisms involved in denitrification included Archaea (1.27%), bacteria (98.68%), and unclassified microorganisms (0.05%). The top four dominant bacterial groups in terms of abundance were Chloroflexota, Acidobacteriota, Deltaproteobacteria, and Bacteria. The abundance of Chloroflexota in the CK, NB15, NB45, FB15, and FB45 treatments was 10.89%, 10.15%, 9.71%, 12.16%, and 10.74%, respectively. As shown in Figure 3g, comparison revealed that at 15 t·ha^{-1}, NB plots displayed a lower Chloroflexota abundance than FB plots ($p < 0.05$); the abundance in NB45 was also lower than in FB15 ($p < 0.01$). The abundance proportions of Acidobacteriota in the CK, NB15, NB45, FB15, and FB45 treatments were 8.44%, 5.99%, 5.01%, 7.96%, and 7.02%, respectively. According to the multiple-group comparison (Figure 3i), the abundance in the NB45 treatment group was significantly lower than that in the control group ($p < 0.01$). For both application durations, a significant decrease in abundance was observed when the biochar rate increased from 15 to 45 t·ha^{-1}. The abundance of Bacteria in the CK, NB15, NB45, FB15, and FB45 treatments was 5.58%, 5.23%, 4.68%, 5.55%, and 5.90%, respectively. Under the high biochar rate (45 t·ha^{-1}), NB conditions led to a significantly lower ($p < 0.01$) relative abundance of Bacteria compared to FB conditions (Figure 3j). Statistical analysis revealed that the NB45 treatment differed significantly from the control (CK) at the $p < 0.05$ level.

3.4. Normalized Stochasticity Ratio (NST) Analysis of the Community Structure of Nitrification and Denitrification in Paddy Field Soil

NST analysis was performed to understand the changes in the community structure of microorganisms related to nitrification and denitrification. As shown in Figure 4a, when the different treatments were compared, there were significant differences in the changes in the community structure of microorganisms related to nitrification. Among them, the NST value of the FB15 treatment was 0.5163, indicating that the construction of the microbial community at this time was mainly dominated by a stochastic process. The NST values of the CK, NB15, NB45, and FB45 treatments were 0.4632, 0.4213, 0.4896, and 0.3934, respectively, indicating that the deterministic process had the greatest impact on the microbial community structure in the FB45 treatment. Significant differences were exhibited in the community structure of denitrifying microorganisms among treatments, as determined by NST analysis. The weakest deterministic effect (NST = 0.4876) on community shifts was observed under NB conditions at the 45 t·ha^{-1} biochar rate. In the FB treatment, the deterministic process of the microbial community structure under the FB15 treatment was the most pronounced, with an NST value of 0.2803.

3.5. Microbial Function Analysis of Nitrification and Denitrification in Paddy Field Soil

As shown in Figure 5a, the functions of the microorganisms related to nitrification were classified and clustered using the KEGG database. The classification level referred to the functions with the top 50 total abundances. The results indicated the presence of five metabolic pathways: nitrogen metabolism, metabolic pathways, microbial metabolism in diverse environments, and carbon and methane metabolism. Among the detected metabolic pathways, the functional abundances of nitrogen, metabolic, and microbial metabolisms in diverse environments were relatively high. After conducting a cluster analysis of all treatments, the treatments under the FB and NB conditions were found to belong to the same hierarchical level. Functional similarity was higher under similar conditions. The functional similarity of the CK treatment was closer to that of the treatments under FB conditions. When comparing the abundance of nitrogen metabolism functions among all treatments, the NB45 and NB15 treatments were relatively weaker.

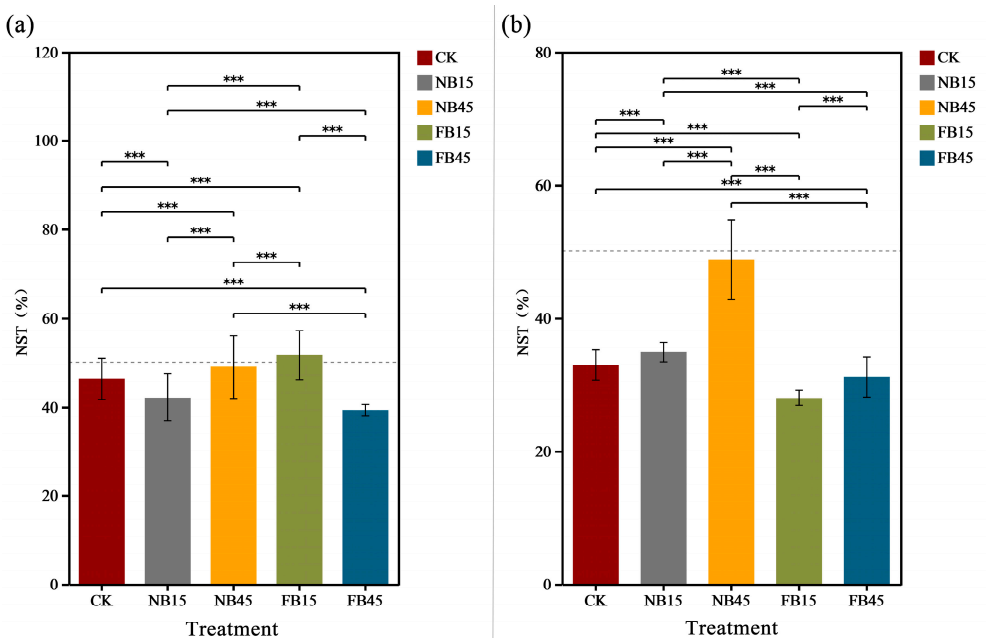


Figure 4. Normalized stochasticity ratio (NST) analysis of nitrifying (**a**) and denitrifying (**b**) microbial communities. CK: control (no biochar); FB15 & FB45: received 15 or 45 t·ha^{-1} biochar in the 8th year (FB); NB15 & NB45: received 15 or 45 t·ha^{-1} biochar in the 1st year (NB). Dashed line shows the 50% NST threshold, above which stochastic processes dominate, below which deterministic processes dominate. ***: significant at $p < 0.001$.

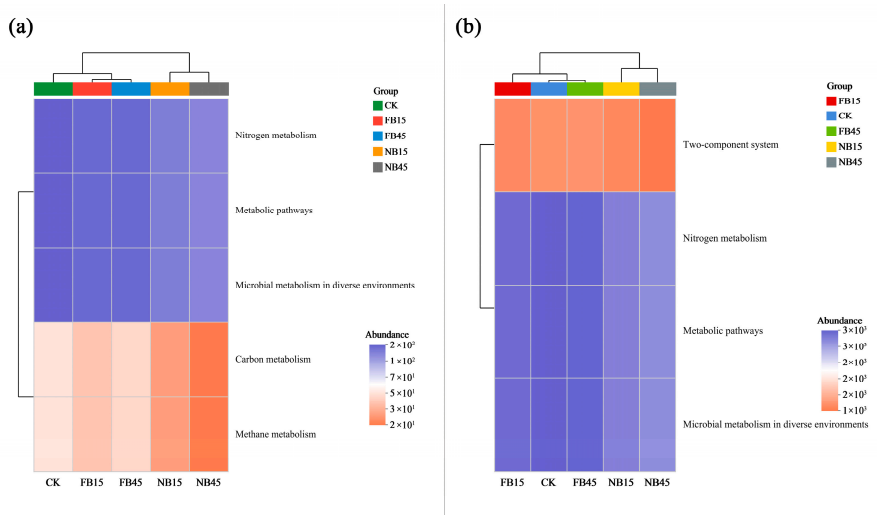


Figure 5. Metabolic functions and cluster analysis of microorganisms involved in nitrification (**a**) and denitrification (**b**). CK: unamended control; FB15 & FB45: received 15 or 45 t·ha^{-1} biochar in the 8th year (FB); NB15 & NB45: received 15 or 45 t·ha^{-1} biochar in the 1st year (NB).

As shown in Figure 5b, there are four metabolic pathways for denitrifying microorganisms in diverse environments: a two-component system, nitrogen metabolism, metabolic pathways, and microbial metabolism. After cluster analysis, the CK and the FB45 treatment groups were found to be at the same hierarchical level and the NB15 and NB45 treatment groups were at the same hierarchical level. Functional similarity was relatively high at the same level of the hierarchy. At the second hierarchical level, the functions of the FB15 treatment group were similar to those of the CK and FB45 treatment groups. When comparing the abundance of nitrogen metabolism functions among all treatments, the abundance under the NB conditions was relatively low.

3.6. Comparison and Differential Analysis of the Microbial Functions of Nitrification and Denitrification in Paddy Field Soil

As shown in Figure 6, principal coordinate analysis (PCoA) and ANOSIM were performed on the functions of the microorganisms related to nitrification. As shown in Figure 6b, the inter-group differences in nitrification-related microbial functions significantly exceeded the intra-group differences (R = 0.571852, p = 0.005). Subsequently, PCoA was performed (Figure 6a). PC1 accounted for 94.07% and PC2 accounted for 2.80%. Based on the degree of clustering, the microbial functional profiles in the CK, FB15, and FB45 treatments were more similar to one another. The similarity between the CK and FB45 treatments was high, and the functional effects of the NB15 and NB45 treatments were relatively similar. Similarly, ANOSIM was applied to assess functional profiles of denitrifying microorganisms (Figure 6d). The analysis revealed significantly greater functional variation between groups compared to within groups (R = 0.546667, p = 0.002). Subsequently, based on the above results, PCoA analysis was conducted (Figure 6c), with PC1 accounting for 97.59% and PC2 accounting for 1.18%. All the treatments were divided into two groups according to their degree of functional similarity. The functional effects of the CK, FB15, and FB45 treatments were relatively similar, as were the functional effects of the treatments under NB conditions. PCoA analysis revealed that sample points from the NB treatment clustered distinctly on the right side of the coordinate axes, while those from the control (CK) and FB treatments concentrated on the left side, indicating that the NB treatment significantly altered the microbial community structure. The exceptionally high variance explained by PC1 (>90%) confirms that the newly applied biochar in this experiment was the primary driver influencing the functional activity of nitrifying and denitrifying microorganisms, accounting for the vast majority of differences observed between samples.

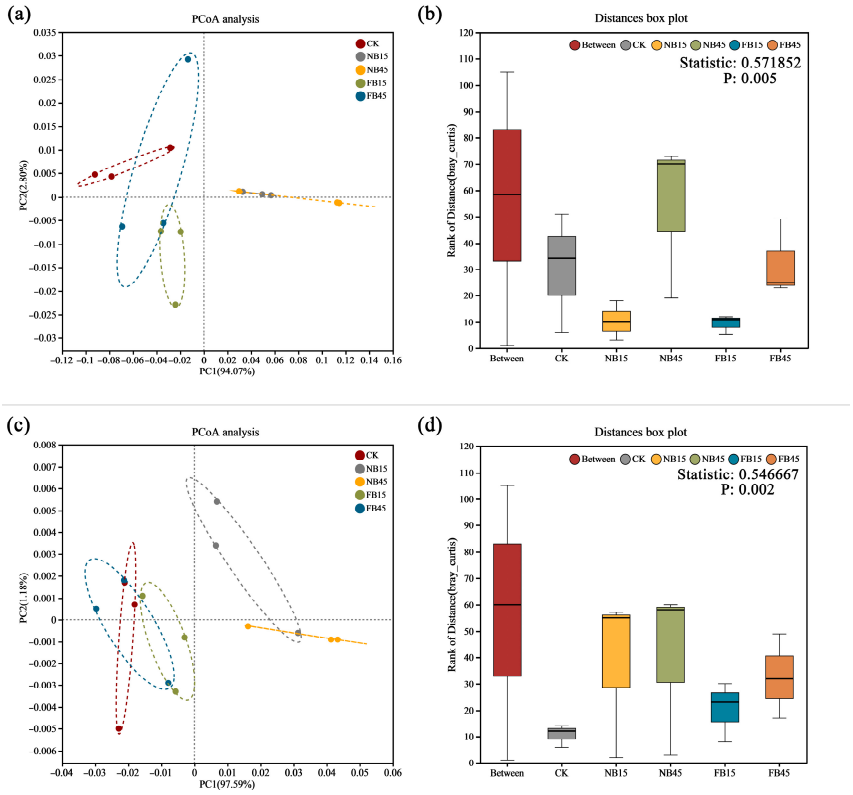


Figure 6. PCoA-based comparison of microbial functions involved in nitrification (**a**) and denitrification (**c**); ANOSIM analysis of microorganisms involved in nitrification (**b**) and denitrification (**d**). CK: unamended control; FB15 & FB45: received 15 or 45 t·ha^{-1} biochar in the 8th year (FB); NB15 & NB45: received 15 or 45 t·ha^{-1} biochar in the 1st year (NB).

3.7. Comparison of Nitrogen Metabolism Functions Among Microbial Groups Related to Nitrification and Denitrification

To elucidate how biochar application duration and rate influence nitrogen metabolism functions, we performed an independent intergroup comparison of these functions in nitrifying and denitrifying microorganisms. Figure 7a presents a comparison of nitrogen metabolism functional profiles across microbial groups associated with nitrification. The analysis revealed that treatments under NB conditions displayed significant functional differences relative to the CK. However, the results for the FB condition showed the opposite. These differences were particularly pronounced under the 45 t·ha^{-1} biochar application rate, with statistical significance at $p < 0.01$. The NB45 treatment significantly outperformed all FB treatments in terms of nitrogen metabolism ($p < 0.05$). As shown in Figure 7b, there were evident differences in the nitrogen metabolism functions among the microbial groups related to denitrification. Relative to the CK, the NB condition showed a significant weakening in nitrogen metabolism functions ($p < 0.05$). In contrast, the functional efficacy was markedly enhanced in the FB15 treatment compared to the NB treatment ($p < 0.05$).

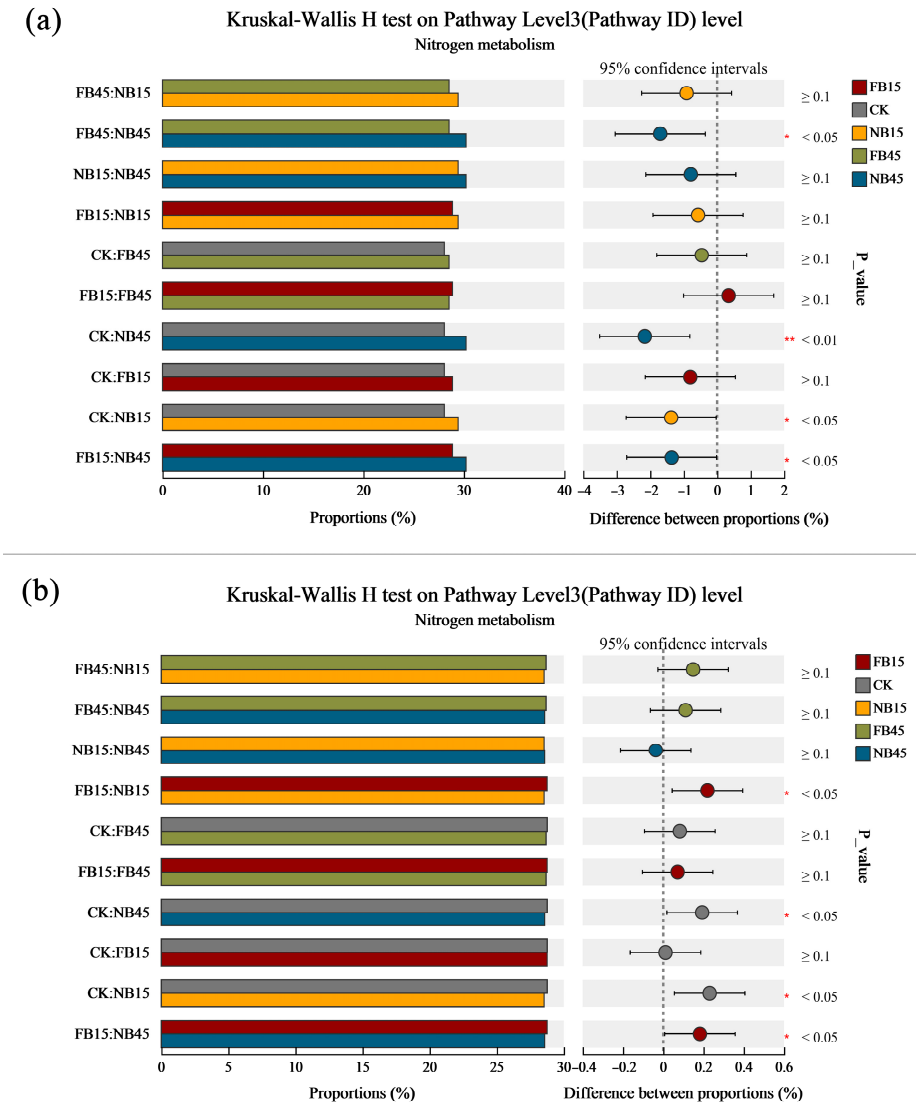


Figure 7. Comparison of the differences in nitrogen metabolism among microbial groups related to nitrification (**a**) and denitrification (**b**). CK: unamended control; FB15 & FB45: received 15 or 45 t·ha^{-1} biochar in the 8th year (FB); NB15 & NB45: received 15 or 45 t·ha^{-1} biochar in the 1st year (NB). *: significant at $p < 0.05$; **: significant at $p < 0.01$.

3.8. Correlation Analysis Between Microorganisms Related to Nitrification and Denitrification and Environmental Factors

Using correlation analysis methods, this study investigated the interactions between microbial species related to nitrification and denitrification processes and environmental factors. Correlation analysis revealed distinct linkages between SOM and nitrifying microbial communities (Figure 8a): positive for all FB treatments ($p < 0.05$) but negative for all others ($p < 0.05$). In the denitrification analysis (Figure 8b), only plots receiving 45 t·ha^{-1} biochar exhibited a positive (though non-significant, $p \geq 0.05$) relationship with pH, whereas negative relationships characterized the remaining treatments. The NO_3^-–N content showed only a positive relationship with the NB15 treatment ($p \geq 0.05$) and the results of its correlation with other treatments were in the opposite direction ($p \geq 0.05$). A positive correlation existed between NH_4^+-N content and the CK and NB15 treatments ($p < 0.05$), while correlations with other treatments were negative ($p < 0.05$). For denitrification-associated microbes (Figure 8b), a positive correlation with soil pH was found under NB conditions at both biochar rates ($p < 0.05$); in contrast, all other treatments showed a negative correlation with pH ($p < 0.05$). At the 15 t·ha^{-1} biochar application rate, a positive correlation ($p \geq 0.05$) was observed solely between SOM and the species composition of denitrifying microorganisms. During the analysis of the contents of NO_3^-–N and NH_4^+–N, no clear patterns were discernible. The NB15, FB45, and CK treatments exhibited positive correlations with NO_3^-–N content ($p \geq 0.05$). Positive correlations with soil NH_4^+–N content were also observed for the NB15 and FB45 treatments ($p \geq 0.05$).

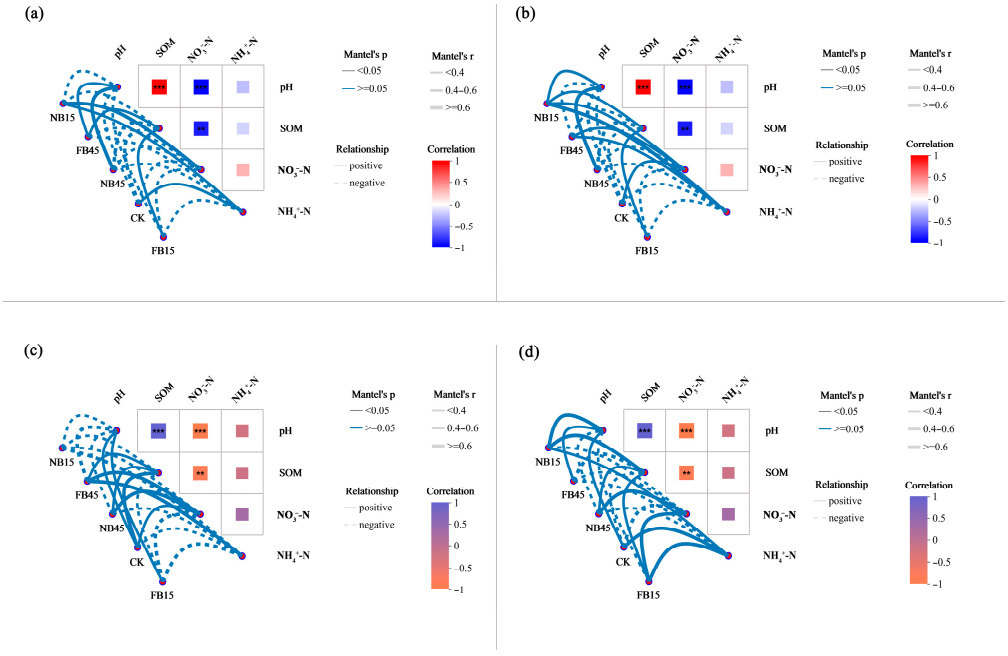


Figure 8. Mantel test network heatmap analysis of microbial community composition for nitrification (**a**) and denitrification (**b**) and their associations with environmental factors; Mantel test network heatmap analysis of microbial community function for nitrification (**c**) and denitrification (**d**) in relation to environmental factors. CK: unamended control; FB15 & FB45: received 15 or 45 t·ha^{-1} biochar in the 8th year (FB); NB15 & NB45: received 15 or 45 t·ha^{-1} biochar in the 1st year (NB). **: significant at $p < 0.01$; ***: significant at $p < 0.001$.

Considering the impact of environmental factors on the functions of microorganisms associated with nitrification and denitrification, a correlation analysis linking these functions to environmental factors was conducted. In the correlation analysis pertaining to nitrification (Figure 8c), the NB15 treatment showed negative correlations with all measured

soil factors: pH, SOM, NO_3^-–N, and NH_4^+–N ($p \geq 0.05$). The FB45 treatment exhibited positive correlations with SOM, NO_3^-–N, and NH_4^+–N ($p \geq 0.05$); however, a negative correlation with pH was observed for this treatment ($p \geq 0.05$). For the NB45 treatment, the correlation pattern was more complex, with positive associations found for SOM and NO_3^-–N ($p \geq 0.05$) but negative associations for pH and NH_4^+–N ($p \geq 0.05$). The CK treatment demonstrated a negative correlation with the content of NH_4^+–N ($p < 0.05$). A positive correlation was found exclusively between the FB15 treatment and the SOM content ($p \geq 0.05$). As shown in Figure 8d, no clear patterns emerged from the correlation analysis of denitrification under comparable circumstances. The different treatments exhibited distinct correlation patterns. Specifically, pH, soil organic matter (SOM), and ammonium nitrogen (NH_4^+–N) were all positively correlated with the NB15 treatment ($p \geq 0.05$). The FB45 treatment and pH were the only variables that exhibited a positive correlation ($p < 0.05$). The NB45 treatment showed a positive correlation with both soil SOM and NO_3^-–N content ($p \geq 0.05$). The CK treatment showed a positive correlation with both the soil pH and NH_4^+–N content ($p < 0.05$). Conversely, a negative correlation with pH was unique to the FB15 treatment ($p < 0.05$).

4. Discussion

4.1. Modulation of Soil Physicochemical Properties by Biochar Application Duration

Biochar, as an emerging soil conditioner, can be applied to soil to achieve sustainable agriculture. The biochar used in this study is prepared from agricultural waste, containing minimal hazardous waste and thus suitable for soil application [38,39]. In this study, the soil pH in the biochar treatment changed significantly. Compared to CK, the application of biochar significantly increased the soil pH. The more pronounced effect under NB relative to FB conditions aligns with the results reported by [40]. For the same application duration, the increase in soil pH became more pronounced with higher biochar application rates; compared to CK, NB45 increased pH by 11.52% and FB45 by 3.99%, both exceeding the pH increase achieved by applying 15 tons of biochar over the same period, which validates the conclusions of a previous study [41]. The underlying mechanism behind this phenomenon lies in the fact that the alkaline components inherent in biochar release a large quantity of exchangeable cations upon entering the soil, thereby accelerating the depletion of protons within the soil. This effectively neutralizes the acidity and elevates the pH levels. Within the optimal application range, a positive correlation exists between soil pH and the amount of carbon applied, as shown in previous studies [42,43]. However, conclusions regarding this matter are not entirely consistent. Some studies have failed to observe a significant pH-raising effect from biochar [44]. This may be related to multiple factors, including the application rate of biochar and its degree of stabilization within the soil. However, the specific underlying mechanisms require further investigation. Additionally, the soil SOM content was significantly increased by the application of biochar, which is consistent with previous findings in rice-wheat rotation systems [45]. The results of this study show that under NB conditions, there was a greater impact on SOM compared to CK, and 45 $t \cdot ha^{-1}$ increased it by 20.51% over 15 $t \cdot ha^{-1}$. The observation that SOM content was higher at 45 $t \cdot ha^{-1}$ than at 15 $t \cdot ha^{-1}$ aligns with earlier findings [21]. In the 8th year after biochar application to the soil, biochar still increased the soil SOM content. During the observation period of this study, the soil NO_3^-–N content exhibited significant fluctuations. The highest NO_3^-–N content was observed under the CK condition, reaching 13.85 $mg \cdot kg^{-1}$, while all biochar treatments significantly reduced it, consistent with findings reported in the literature [46,47]. Some studies also showed that the addition of biochar had no significant effect on the soil NO_3^-–N content [48]. Moreover, the content of NH_4^+–N in soil after biochar application decreases significantly [49–51], and the observational data

from this study are consistent with this conclusion. This may be because, after biochar is applied to the soil, an oxidation reaction occurs, which improves its cation adsorption capacity and reduces the anion exchange capacity. This led to an increase in the cation value of biochar with an increase in the number of years of application. In soils where biochar has been applied for a long time, the NH_4^+–N content is higher than that in the first year of biochar application [52,53]. The observed reduction in ammonium nitrogen content in this study, differing from the simple expectation of "adsorption leading to accumulation," reveals the complexity of biochar's effects. This may occur because biochar enhances microbial immobilization of NH_4^+, thereby increasing soil NH_4^+ consumption and indirectly reducing NO_3^- production [20]. Although measured concentrations in the soil inorganic nitrogen pool decrease, nitrogen is temporarily "locked" within living microbial cells, reducing the risk of leaching. The differing adsorption capacities of biochar toward NH_4^+ across various application durations also influence N_2O emissions to some extent [18,20]. Future studies may monitor soil NH_4^+ dynamics and biochar adsorption capacity to distinguish the relative contributions of these two mechanisms. It should be noted that this study primarily focuses on the effects of biochar application in the field, lacking comparative data on the characterization of fresh versus aged biochar. This may be a key reason for the difference in FB and NB effects. Future research should incorporate detailed material characterization to clarify the underlying mechanism. Overall, biochar continued to exert regulatory effects on soil physicochemical properties even eight years after application.

4.2. Effects of the Application Duration of Biochar on N_2O Emissions from Paddy Fields

This study employed a sampling frequency of once every 7 days, with an additional measurement 3 days after fertilization. While this approach aligns with conventional practices in similar studies, it may not fully capture the sustained, transient peaks of extremely high N_2O emissions that occur following fertilization and rainfall events. Consequently, the seasonal cumulative N_2O emissions reported in this study may represent a conservative estimate. Future high-frequency continuous monitoring (e.g., using automated chambers) will facilitate more precise quantification of N_2O emission peaks. Divergent conclusions exist in the literature regarding biochar's impact on N_2O emissions. The literature presents a dichotomy regarding biochar's impact on N_2O emissions. While a body of work supports its mitigating role [29,30,54,55], other studies have recorded neutral or even stimulatory effects [56]. The observational data from this study indicate that in the first year following the application of biochar to the soil, there were two trends in the impact on N_2O emissions. Compared to CK, under a high biochar application rate, N_2O emissions increased, and cumulative emissions increased by 18.44%, whereas under a low biochar application rate, N_2O emissions decreased significantly by 54.56%, a conclusion supported by [57]. This inconsistency in N_2O emissions may be related to the application rate of biochar and pyrolysis temperature, with the specific reasons requiring further in-depth research and verification. In the eighth year after biochar application to rice fields, N_2O emissions under the two treatments were alleviated, and the cumulative emissions tended to be consistent. FB15 and FB45 decreased by 21.42% and 24.77%, respectively, with no evident difference. This observation aligns with [58], who reported that biochar alleviates N_2O emissions after two to four years of application in paddy fields. Biochar limits substrate supply for denitrification by adsorbing inorganic nitrogen (NO_3^-–N and NH_4^+–N) on its surface, ultimately suppressing soil N_2O emissions [59]. This study investigated the impact of biochar on N_2O emissions based on two dimensions—application duration and dosage—with the aim of providing theoretical support for investigating the sustainability of its emission reduction effects.

4.3. Effects of the Application Duration of Biochar on Nitrifying and Denitrifying Microorganisms

In rice paddy ecosystems, the principal sources of N_2O are the microbial processes of nitrification and denitrification [60]. Previous research indicates that amending soil with biochar stimulates the proliferation of nitrifying microbes (e.g., ammonium-oxidizing bacteria) and alters the community composition of denitrifiers [61–63]. Similarly, the species analysis conducted in this study under NB and FB regimes showed comparable patterns in the relative abundances of nitrifier and denitrifier communities. Elevated levels of SOM content and soil pH were associated with biochar application. These changes in the soil environment may further influence the abundance of nitrifying and denitrifying microbial communities. Furthermore, biochar enhances the efficiency of electron transfer within the soil system, thereby promoting the ability of denitrifying microorganisms to reduce N_2O and drive its conversion to N_2 [64].

Based on the NST analysis of the changes in the community structure of nitrification and denitrification, it was found that during nitrification and denitrification, the community structure of FB15 underwent the most significant changes. However, no patterns were found, possibly owing to differences in the duration and amount of biochar application. This may also be because only one type of raw material was used to prepare the biochar. The raw materials used to prepare biochar and the pyrolysis conditions can affect the biogeochemical action of biochar in soil [65]. Further research in this area is warranted. After comparison with the KEGG database, the metabolic pathways were determined. According to the functional abundance values, when the duration of biochar application was the same, the functions of the microorganisms related to nitrification and denitrification were similar. Eight years after application, functional similarity increased between the control and biochar-treated soils. Nitrogen metabolism functions in nitrifier-associated communities were more pronounced under NB conditions than under FB conditions. Conversely, denitrifier-linked nitrogen metabolism exhibited enhanced expression in FB treatments compared to NB treatments. This indicates that although biochar continued to have an effect in the eighth year of application, its effectiveness weakened over time. However, the high-dose treatment (45 $t \cdot ha^{-1}$) used in this study was primarily designed to maximize effects under experimental conditions and reveal potential mechanisms, rather than representing a recommended practical agronomic application rate. Based on the findings of this study, future research should validate the long-term effects of fresh versus aged biochar at application rates closer to real-world production conditions. Additionally, systematic integrated assessments of cost, benefits, and environmental impacts should be conducted to develop truly scalable application protocols.

5. Conclusions

Based on a field experiment, the application duration of biochar directly affected N_2O emissions and the associated functional changes in microorganisms in paddy soils. The organic matter content of paddy soil was increased by fresh, high-level biochar (e.g., NB45). In contrast, aged, high-level biochar (e.g., FB45) reduced the soil's NO_3^-–N content. Biochar reduced N_2O emissions (except for NB45) and influenced microbial functions related to nitrification and denitrification in paddy fields. The effects of biochar vary with application duration and rate. The influence of fresh biochar (NB) on SOM and pH was more pronounced compared to that of aged biochar (FB). In particular, NB45 increased SOM and pH by 55.26% and 11.52%, respectively. Fresh biochar (NB) had a higher NO_3^-–N content than aged biochar (FB), but the NH_4^+–N content was exactly the opposite of that of nitrate nitrogen. As the duration of biochar application increased, the effectiveness of biochar in reducing N_2O emissions decreased. NB15 reduced the cumulative N_2O emissions by 54.56%. NB enhanced the nitrogen metabolism functions

of microorganisms related to nitrification, while suppressing those of microorganisms associated with denitrification. Considering both emission reduction and soil improvement benefits, applying 15 t·ha^{-1} of fresh (NB) biochar represents the optimal application rate. In conclusion, biochar continued to exert its effects on soil nutrients and GHG emissions even eight years after application. However, the combined application of fresh and aged biochar in paddy field ecosystems, particularly its optimal application rate range, long-term effects, and ecological benefits, warrants further investigation. To understand potential long-term negative consequences, it is critical to ensure sustainability. This study provides a theoretical foundation for establishing an agricultural circular economy and enhancing the environmental benefits of agricultural production in cold regions.

Author Contributions: Z.Z.: Writing—Original Draft, Writing—Review and Editing, Conceptualization, Methodology, and Investigation. X.L.: Writing—Original Draft, Writing—Review and Editing, Formal analysis, and Investigation. K.Z.: Visualization, Writing—Review and Editing, and Data Curation. J.Z.: Writing—Review and Editing, Supervision, and Visualization. Y.S.: Writing—Review and Editing, Supervision, and Formal analysis. X.B.: Investigation, Software, and Data Curation. Z.S.: Writing—Review and Editing, Supervision, and Visualization. J.W.: Investigation, Software, and Data Curation. W.Z.: Writing—Review and Editing, Methodology, and Supervision. J.G.: Writing—Review and Editing, Methodology, Conceptualization, Project administration, and Funding acquisition. All authors have read and agreed to the published version of the manuscript.

Funding: The authors are grateful for the financial support received from the Natural Science Foundation of Liaoning Province (No. 2025-MS-165), the National Natural Science Foundation of China (No. 31501250), the Liaoning Province Science and Technology Major Project (No. 2024JH1/11700006-4-2), and the Liaoning Revitalization Talents Program (No. XLYC2007169).

Data Availability Statement: The original contributions presented in this study are included in the article. Further inquiries can be directed to the corresponding author.

Conflicts of Interest: The authors declare that they have no known competing financial interests or personal relationships that could have appeared to influence the work reported in this paper.

References

1. Gu, D.M.; Liu, Y.W.; Zhao, W.G.; Qiu, S.T.; Cui, N.; Hu, X.Y.; Zhao, P. Status of Research on Greenhouse Gas Emissions from Wastewater Collection Systems. *Water* **2023**, *15*, 2512. [CrossRef]
2. Sainova, G.; Yessenbayeva, Z.; Akbasova, A.; Tastambek, K.; Hanc, A. An Effective Melon Fly Control Strategy Based on Disinfection and Soil Productivity Management. *Sustainability* **2023**, *15*, 16033. [CrossRef]
3. Li, L.D.; Awada, T.; Shi, Y.Y.; Jin, V.L.; Kaiser, M. Global Greenhouse Gas Emissions From Agriculture: Pathways to Sustainable Reductions. *Glob. Change Biol.* **2025**, *31*, e70015. [CrossRef]
4. Qi, R.Y.; Dong, J.H.; Kang, Y.; Xie, H.J.; Wu, H.M.; Hu, Z.; Guo, Z.Z. Migration and Transformation of Greenhouse Gases in Constructed Wetlands: A Bibliometric Analysis and Trend Forecast. *Water* **2025**, *17*, 412. [CrossRef]
5. Huang, Y.; Deng, M.; Zhou, S.; Xue, Y.; Yeerken, S.; Wang, Y.; Li, L.; Song, K. Microbial mechanisms underlying the reduction of N_2O emissions from submerged plant covered system. *Water Res. X* **2025**, *28*, 100314. [CrossRef]
6. Rahman, M.S.; Ferdous, J.; Mumu, N.J.; Kamruzzaman, M.; Eckhardt, C.; Zaman, M.; Müller, C.; Jahangir, M.M.R. Crop residues integration with nitrogen rates reduces yield-scaled nitrous oxide emissions and improves maize yield and soil quality. *J. Integr. Environ. Sci.* **2024**, *21*, 2310856. [CrossRef]
7. Huan, S.H.; Liu, X.L. Machine learning-driven analysis of greenhouse gas emissions from rice production in major Chinese provinces: Identifying key factors and developing reduction strategies. *Eur. J. Agron.* **2025**, *164*, 127536. [CrossRef]
8. Yuan, B.Z.; Sun, J. Research trend of rice and greenhouse gases based on Web of Science: A bibliometric analysis. *All Earth* **2023**, *35*, 16–30. [CrossRef]
9. Khatibi, S.M.H.; Borbe, M.A.A.; Dimaano, N.G.; Radanielson, A.M.; Ali, J. Advanced technologies for reducing greenhouse gas emissions from rice fields: Is hybrid rice the game changer? *Plant Commun.* **2025**, *6*, 101224. [CrossRef] [PubMed]
10. Lu, Y.X.; Yin, B.F.; Li, Y.G.; Zang, Y.X.; Zhou, X.; Zhang, Y.M. Snow and nitrogen manipulation do not alter the dominant role of fungi in the N_2O production of biocrusts in a temperate desert. *Appl. Soil Ecol.* **2025**, *205*, 105766. [CrossRef]

11. Beristain-Cardoso, R.; Gómez, J.; Méndez-Pampín, R. The behavior of nitrifying sludge in presence of sulfur compounds using a floating biofilm reactor. *Bioresour. Technol.* **2010**, *101*, 8593–8598. [CrossRef]
12. Stein, L.Y. Insights into the physiology of ammonia-oxidizing microorganisms. *Curr. Opin. Chem. Biol.* **2019**, *49*, 9–15. [CrossRef] [PubMed]
13. Wrage-Mönnig, N.; Horn, M.A.; Well, R.; Müller, C.; Velthof, G.; Oenema, O. The role of nitrifier denitrification in the production of nitrous oxide revisited. *Soil Biol. Biochem.* **2018**, *123*, A3–A16. [CrossRef]
14. Wang, T.; Ji, C.Y.; Zhou, W.; Chen, H.; Chen, Y.; Liu, Q.; Cao, T.; Yang, Z.P.; Fu, Y.; Yue, X.P.; et al. Dry season residual straw reduces nitrous oxide emissions during rice season in upland-paddy rotation systems by inhibiting soil denitrification. *Biol. Fertil. Soils* **2024**, *61*, 627–640. [CrossRef]
15. Tang, Y.J.; Su, X.X.; Wen, T.; McBratney, A.B.; Zhou, S.Y.D.; Huang, F.Y.; Zhu, Y.G. Soil properties shape the heterogeneity of denitrification and N_2O emissions across large-scale flooded paddy soils. *Glob. Change Biol.* **2024**, *30*, e17176. [CrossRef]
16. Antonio, C.H.; David, C.G.; Jesús, G.L.; Bedmar, E.J. Effect of nitrogen fertilisers on nitrous oxide emission, nitrifier and denitrifier abundance and bacterial diversity in closed ecological systems. *Appl. Soil Ecol.* **2020**, *145*, 103380. [CrossRef]
17. Deng, X.Z.; Xu, T.T.; Zhang, F.Q.; Xue, L.H.; Yang, L.Z.; Hou, P.F. Effects of warming and fertilization on nirK-, nirS- and nosZ-type denitrifier communities in paddy soil. *Sci. Total Environ.* **2024**, *955*, 177057. [CrossRef]
18. Zhou, Y.C.; Zhao, Z.L.; Li, D.Y.; Wang, Y.P.; Yang, J.R.; Han, W.; Li, S. Effects of aged biochar additions at different addition ratios on soil greenhouse gas emissions. *Sci. Total Environ.* **2024**, *955*, 176914. [CrossRef]
19. Bhujbal, S.K.; Ghosh, P.; Vijay, V.K. Modeling and optimization of biomethanation of rice straw with biochar supplementation using response surface methodology and machine learning. *Sustain. Energy Technol. Assess.* **2024**, *71*, 104006. [CrossRef]
20. Xie, Y.; Yang, C.; Ma, E.D.; Tan, H.; Zhu, T.B.; Müller, C. Biochar stimulates NH_4^+ turnover while decreasing NO_3^- production and N_2O emissions in soils under long-term vegetable cultivation. *Sci. Total Environ.* **2020**, 140266. [CrossRef]
21. Zhang, Y.F.; Wang, J.M.; Feng, Y. The effects of biochar addition on soil physicochemical properties: A review. *CATENA* **2021**, *202*, 105284. [CrossRef]
22. Vicente, L.; Peña, D.; Fernández, D.; Albarrán, Á.; Nunes, J.M.R.; Piñeiro, A.L. Alternate wetting and drying irrigation with field aged biochar may enhance water and rice productivity. *Agron. Sustain. Dev.* **2025**, *45*, 6. [CrossRef]
23. Meng, C.B.; Xing, Y.T.; Ding, Y.; Zhang, Q.C.; Di, H.J.; Tang, C.X.; Xu, J.M.; Li, Y. Soil acidification induced variation of nitrifiers and denitrifiers modulates N_2O emissions in paddy fields. *Sci. Total Environ.* **2023**, *882*, 163623. [CrossRef]
24. Wang, L.; Chen, D.J.; Zhu, L.Z. Biochar carbon sequestration potential rectification in soils: Synthesis effects of biochar on soil CO_2, CH_4 and N_2O emissions. *Sci. Total Environ.* **2023**, *904*, 167047. [CrossRef]
25. Chen, H.; Yin, C.; Fan, X.P.; Ye, M.J.; Peng, H.Y.; Li, T.Q.; Zhao, Y.H.; Wakelin, S.A.; Chu, G.X.; Liang, Y.C. Reduction of N_2O emission by biochar and/or 3,4-dimethylpyrazole phosphate (DMPP) is closely linked to soil ammonia oxidizing bacteria and nosZI-N_2O reducer populations. *Sci. Total Environ.* **2019**, *694*, 133658. [CrossRef]
26. Yang, X.Y.; Duan, P.P.; Cao, Y.B.; Wang, K.L.; Li, D.J. Mechanisms of mitigating nitrous oxide emission during composting by biochar and calcium carbonate addition. *Bioresour. Technol.* **2023**, *388*, 129772. [CrossRef]
27. Ji, C.; Han, Z.Q.; Zheng, F.W.; Wu, S.; Wang, J.Y.; Wang, J.D.; Zhang, H.; Zhang, Y.C.; Liu, S.W.; Li, S.Q.; et al. Biochar reduced soil nitrous oxide emissions through suppressing fungal denitrification and affecting fungal community assembly in a subtropical tea plantation. *Agric. Ecosyst. Environ.* **2022**, *326*, 107784. [CrossRef]
28. Wang, Q.R.; Yao, D.X.; Tang, X.Y.; Zhu, D.C.; Sun, Y.Q.; Zhang, H.; Yang, Q.; Yang, H.P.; Chen, H.P.; Mašek, O. Maximizing nitrous oxide mitigation potential of straw-derived biochar in China with optimal application strategies. *Biochar* **2026**, *8*, 1. [CrossRef]
29. Qi, L.; Pokharel, P.; Ni, C.S.; Gong, X.Q.; Zhou, P.; Niu, H.D.; Wang, Z.F.; Gao, M. Biochar changes thermal activation of greenhouse gas emissions in a rice–lettuce rotation microcosm experiment. *J. Clean Prod.* **2020**, *247*, 119148. [CrossRef]
30. Zhao, Y.Z.; Jiang, H.F.; Gao, J.P.; Wan, X.; Yan, B.C.; Liu, Y.; Cheng, G.Q.; Chen, L.Q.; Zhang, W.Z. Effects of biochar application methods on greenhouse gas emission and nitrogen use efficiency in paddy fields. *Sci. Total Environ.* **2024**, *915*, 169809. [CrossRef]
31. Chen, S.F.; Zhou, Y.Q.; Chen, Y.R.; Gu, J. fastp: An ultra-fast all-in-one FASTQ preprocessor. *Bioinformatics* **2018**, *34*, i884–i890. [CrossRef]
32. Li, D.H.; Liu, C.M.; Luo, R.B.; Sadakane, K.; Lam, T.W. MEGAHIT: An ultra-fast single-node solution for large and complex metagenomics assembly via succinct de Bruijn graph. *Bioinformatics* **2015**, *31*, 1674–1676. [CrossRef]
33. Hyatt, D.; Chen, G.-L.; Locascio, P.F.; Land, M.L.; Larimer, F.W.; Hauser, L.J. Prodigal: Prokaryotic gene recognition and translation initiation site identification. *BMC Bioinform.* **2010**, *11*, 119. [CrossRef] [PubMed]
34. Noguchi, H.; Park, J.; Takagi, T. MetaGene: Prokaryotic gene finding from environmental genome shotgun sequences. *Nucleic Acids Res.* **2006**, *34*, 5623–5630. [CrossRef]
35. Fu, L.M.; Niu, B.F.; Zhu, Z.W.; Wu, S.T.; Li, W.Z. CD-HIT: Accelerated for clustering the next-generation sequencing data. *Bioinformatics* **2012**, *28*, 3150–3152. [CrossRef] [PubMed]
36. Li, R.Q.; Li, Y.R.; Kristiansen, K.; Wang, J. SOAP: Short oligonucleotide alignment program. *Bioinformatics* **2008**, *24*, 713–714. [CrossRef] [PubMed]

37. Buchfink, B.; Xie, C.; Huson, D.H. Fast and sensitive protein alignment using DIAMOND. *Nat. Methods* **2015**, *12*, 59–60. [CrossRef]
38. Tsolis, V.; Barouchas, P. Biochar as Soil Amendment: The Effect of Biochar on Soil Properties Using VIS-NIR Diffuse Reflectance Spectroscopy, Biochar Aging and Soil Microbiology—A Review. *Land* **2023**, *12*, 1580. [CrossRef]
39. Xu, L.; Zhao, F.; Peng, J.; Ji, M.; Li, B.L. A Comprehensive Review of the Application and Potential of Straw Biochar in the Remediation of Heavy Metal-Contaminated Soil. *Toxics* **2025**, *13*, 69. [CrossRef]
40. Wang, C.; Chen, D.; Shen, J.L.; Yuan, Q.; Fan, F.L.; Wei, W.X.; Li, Y.; Wu, J.S. Biochar alters soil microbial communities and potential functions 3–4 years after amendment in a double rice cropping system. *Agric. Ecosyst. Environ.* **2021**, *311*, 107291. [CrossRef]
41. Luo, Q.R.; Liu, C.E.; Zhao, Y.Q.; Zhang, W.L.; Chen, J.Q.; Pan, Y.; Duan, C.Q. Influence of biochar on the remediation of cadmium-contaminated soil in an Eisenia fetida–Solanum nigrum system. *Environ. Chem. Ecotoxicol.* **2024**, *6*, 132–143. [CrossRef]
42. Khan, Z.; Zhang, K.K.; Khan, M.N.; Zhu, K.M.; Hu, L.Y. Effects of biochar persistence on soil physiochemical properties, enzymatic activities, nutrient utilization, and crop yield in a three-year rice-rapeseed crop rotation. *Eur. J. Agron.* **2024**, *154*, 127096. [CrossRef]
43. Zhang, K.; Zhang, Z.C.; Sui, Y.H.; Wang, J.L.; Pei, X.B.; Zhao, Y.Z.; Gao, J.P.; Zhang, W.Z. The application years of biochar affect CH_4 emission by negatively methanogens and increased rice yield. *Environ. Technol. Innov.* **2025**, *38*, 104099. [CrossRef]
44. Quilliam, R.S.; Glanville, H.C.; Wade, S.C.; Jones, D.L. Life in the 'charosphere'—Does biochar in agricultural soil provide a significant habitat for microorganisms? *Soil Biol. Biochem.* **2013**, *65*, 287–293. [CrossRef]
45. Xia, H.; Shen, J.; Riaz, M.; Jiang, C.C.; Zu, C.L.; Jiang, C.Q.; Liu, B. Effects of Biochar and Straw Amendment on Soil Fertility and Microbial Communities in Paddy Soils. *Plants* **2024**, *13*, 1478. [CrossRef] [PubMed]
46. Case, S.D.C.; McNamara, N.P.; Reay, D.S.; Whitaker, J. The effect of biochar addition on N_2O and CO_2 emissions from a sandy loam soil—The role of soil aeration. *Soil Biol. Biochem.* **2012**, *51*, 125–134. [CrossRef]
47. Chen, X.; Yang, S.H.; Jiang, Z.W.; Ding, J.; Sun, X. Biochar as a tool to reduce environmental impacts of nitrogen loss in water-saving irrigation paddy field. *J. Clean Prod.* **2021**, *290*, 125811. [CrossRef]
48. Zhou, Y.; Lv, L.; Yu, Z.; Zhang, J.; Wang, B.; Yang, R.D.; Chen, M.; Wu, P.; Wang, S.S. Synergistic effect between biochar and sulfidized nano-sized zero-valent iron enhanced cadmium immobilization in a contaminated paddy soil. *Biochar* **2024**, *6*, 55. [CrossRef]
49. Nguyen, T.T.N.; Xu, C.Y.; Tahmasbian, I.; Che, R.X.; Xu, Z.H.; Zhou, X.H.; Wallace, H.M.; Bai, S.H. Effects of biochar on soil available inorganic nitrogen: A review and meta-analysis. *Geoderma* **2017**, *288*, 79–96. [CrossRef]
50. Zhang, Y.Q.; Hou, R.J.; Fu, Q.; Li, T.X.; Li, M.; Dong, S.Q.; Shi, G.X. Soil environment, carbon and nitrogen cycle functional genes in response to freeze-thaw cycles and biochar. *J. Clean Prod.* **2024**, *444*, 141345. [CrossRef]
51. Gao, J.P.; Zhao, Y.Z.; Zhang, W.Z.; Sui, Y.H.; Jin, D.D.; Xin, W.; Yi, J.; He, D.W. Biochar prepared at different pyrolysis temperatures affects urea-nitrogen immobilization and N_2O emissions in paddy fields. *PeerJ* **2019**, *7*, e7027. [CrossRef]
52. Cayuela, M.L.; Zwieten, L.V.; Singh, B.P.; Jeffery, S.; Roig, A.; Sánchez-Monedero, M.A. Biochar's role in mitigating soil nitrous oxide emissions: A review and meta-analysis. *Agric. Ecosyst. Environ.* **2014**, *191*, 5–16. [CrossRef]
53. Dong, D.; Feng, Q.B.; McGrouther, K.; Yang, M.; Wang, H.L.; Wu, W.X. Effects of biochar amendment on rice growth and nitrogen retention in a waterlogged paddy field. *J. Soils Sediments* **2015**, *15*, 153–162. [CrossRef]
54. Zhao, Y.Z.; Jiang, H.F.; Gao, J.P.; Feng, Y.Y.; Yan, B.C.; Li, K.; Lan, Y.; Zhang, W.Z. Effects of nitrogen co-application by different biochar materials on rice production potential and greenhouse gas emissions in paddy fields in northern China. *Environ. Technol. Innov.* **2023**, *32*, 103242. [CrossRef]
55. Duan, P.P.; Zhang, X.; Zhang, Q.Q.; Wu, Z.; Xiong, Z.Q. Field-aged biochar stimulated N_2O production from greenhouse vegetable production soils by nitrification and denitrification. *Sci. Total Environ.* **2018**, *642*, 1303–1310. [CrossRef] [PubMed]
56. Sun, H.J.; Zhang, Y.; Yang, Y.T.; Chen, Y.D.; Jeyakumar, P.; Shao, Q.L.; Zhou, Y.F.; Ma, M.; Zhu, R.Q.; Qian, Q.W.; et al. Effect of biofertilizer and wheat straw biochar application on nitrous oxide emission and ammonia volatilization from paddy soil. *Environ. Pollut.* **2021**, *275*, 116640. [CrossRef] [PubMed]
57. Zhang, Q.Q.; Wu, Z.; Zhang, X.; Duan, P.P.; Shen, H.J.; Gunina, A.; Yan, X.Y.; Xiong, Z.Q. Biochar amendment mitigated N_2O emissions from paddy field during the wheat growing season. *Environ. Pollut.* **2021**, *281*, 117026. [CrossRef]
58. Jiang, Z.W.; Yang, S.H.; Pang, Q.Q.; Abdalla, M.; Qi, S.T.; Hu, J.Z.; Qiu, H.N.; Smith, P. Optimizing biochar application rate and predicting of climate change impacts on net greenhouse gas emissions in paddy systems using DNDC-BC model. *Agric. For. Meteorol.* **2025**, *364*, 110461. [CrossRef]
59. Liu, C.; Chen, T.T.; Zhang, F.; Han, H.W.; Yi, B.J.; Chi, D.C. Soil carbon sequestration increment and carbon-negative emissions in alternate wetting and drying paddy ecosystems through biochar incorporation. *Agric. Water Manag.* **2024**, *300*, 108908. [CrossRef]
60. Zhang, H.K.; Fang, Y.Y.; Chen, Y.C.; Li, Y.; Lin, Y.X.; Wu, J.S.; Cai, Y.J.; Chang, S.X. Enhanced soil potential N_2O emissions by land-use change are linked to AOB-amoA and nirK gene abundances and denitrifying enzyme activity in subtropics. *Sci. Total Environ.* **2022**, *850*, 158023. [CrossRef]
61. Song, Y.J.; Zhang, X.L.; Ma, B.; Chang, S.X.; Gong, J. Biochar addition affected the dynamics of ammonia oxidizers and nitrification in microcosms of a coastal alkaline soil. *Biol. Fertil. Soils* **2014**, *50*, 321–332. [CrossRef]

62. Chen, G.H.; Zhang, Z.R.; Zhang, Z.Y.; Zhang, R.D. Redox-active reactions in denitrification provided by biochars pyrolyzed at different temperatures. *Sci. Total Environ.* **2018**, *615*, 1547–1556. [CrossRef] [PubMed]
63. Altynbay, N.; Tastambek, K.; Akimbekov, N.; Digel, I.; Tagayev, K.; Kamenov, B.; Liu, X.R. A Comprehensive Review on Enhancing Saline Soil Reclamation Efficiency through Bacterial Solubilization of Low-Rank Coal. *Eng. Sci.* **2024**, *30*, 1147. [CrossRef]
64. Chen, J.H.; Liu, X.Y.; Li, L.Q.; Zheng, J.W.; Qu, J.J.; Zheng, J.F.; Zhang, X.H.; Pan, G.X. Consistent increase in abundance and diversity but variable change in community composition of bacteria in topsoil of rice paddy under short term biochar treatment across three sites from South China. *Appl. Soil Ecol.* **2015**, *91*, 68–79. [CrossRef]
65. Feng, Q.W.; Wang, B.; Zimmerman, A.R.; Wu, P.; Lee, X.Q.; Chen, M.; Zhang, J. Application of C and N isotopes to the study of biochar biogeochemical behavior in soil: A review. *Earth-Sci. Rev.* **2024**, *256*, 104860. [CrossRef]

Disclaimer/Publisher's Note: The statements, opinions and data contained in all publications are solely those of the individual author(s) and contributor(s) and not of MDPI and/or the editor(s). MDPI and/or the editor(s) disclaim responsibility for any injury to people or property resulting from any ideas, methods, instructions or products referred to in the content.